tect plants from infection by strain 4091-5-8 at 0.5 mg/ml.
16. E. Loumaye, J. Thorner, K. J. Catt, *Science* **218**, 1323 (1982).
17. Abbreviations for the amino acid residues are: A, Ala; C, Cys; D, Asp; G, Gly; H, His; I, Ile; K, Lys; L, Leu; M, Met; N, Asn; P, Pro; Q, Gln; S, Ser; V, Val; W, Trp; and Y, Tyr.
18. Strains were generously provided by B. Valent of DuPont, Wilmington, DE, and J. Becker of the University of Tennessee, Knoxville. We thank S. McBride for technical assistance and B. Valent and J. E. Hamer for providing research materials and encouragement to work with *M. grisea*. We also thank J. Becker and D. Cook for helpful discussions. Support for this work was provided by funds from USPHS grant R29GM47977, the Texas Rice Research Foundation, the Texas Advanced Research Program (D.J.E.), and USPHS grant GM22086 (F.N).

14 November 1996; accepted 21 March 1997

Effectiveness of Anthracycline Against Experimental Prion Disease in Syrian Hamsters

F. Tagliavini,* R. A. McArthur, B. Canciani, G. Giaccone, M. Porro, M. Bugiani, P. M.-J. Lievens, O. Bugiani, E. Peri, P. Dall'Ara, M. Rocchi, G. Poli, G. Forloni, T. Bandiera, M. Varasi, A. Suarato, P. Cassutti, M. A. Cervini, J. Lansen, M. Salmona, C. Post

Prion diseases are transmissible neurodegenerative conditions characterized by the accumulation of protease-resistant forms of the prion protein (PrP), termed PrPres, in the brain. Insoluble PrPres tends to aggregate into amyloid fibrils. The anthracycline 4′-iodo-4′-deoxy-doxorubicin (IDX) binds to amyloid fibrils and induces amyloid resorption in patients with systemic amyloidosis. To test IDX in an experimental model of prion disease, Syrian hamsters were inoculated intracerebrally either with scrapie-infected brain homogenate or with infected homogenate coincubated with IDX. In IDX-treated hamsters, clinical signs of disease were delayed and survival time was prolonged. Neuropathological examination showed a parallel delay in the appearance of brain changes and in the accumulation of PrPres and PrP amyloid.

Prion diseases, such as scrapie of sheep, spongiform encephalopathy of cattle, and Creutzfeldt-Jakob disease of humans, are transmissible neurodegenerative conditions characterized by the accumulation of protease-resistant forms of the prion protein (PrP), termed PrPres, in the brain (*1*). Unlike the normal PrP, PrPres has a large amount of β-sheet secondary structure and a strong tendency to aggregate into amyloid fibrils (*2*). Deposition of PrPres and PrP amyloid is accompanied by nerve cell degeneration and glial cell proliferation, leading to the clinical signs of disease (*3*). In scrapie-infected hamsters, survival time is prolonged by the amyloid-binding dye Congo red (*4*). Congo red inhibits the accumulation of PrPres in scrapie-infected neuroblastoma cells without affecting the metabolism of normal PrP (*5*).

The anthracycline 4′-iodo-4′-deoxy-doxorubicin (IDX) (Fig. 1A) is a recently developed derivative of doxorubicin, a drug of proven efficacy in a large number of malignancies (*6*). The administration of IDX to eight patients with plasma cell dyscrasias complicated by immunoglobulin light-chain amyloidosis resulted in the partial resorption of amyloid deposits in three cases. In addition, four of the eight patients exhibited discernible clinical improvement, two patients showed reduced symptoms of the disease, and the other two patients were rendered stable (*7*). This unexpected activity of the compound was confirmed by further studies showing that IDX binds strongly to amyloid fibrils of different chemical composition, inhibits in vitro assembly of insulin into amyloid fibrils, and reduces amyloid deposits in a murine model of reactive amyloidosis (*8*). Thus, IDX can be regarded as a prototype of a class of drugs that are able to inhibit amyloidogenesis, reverse tissue deposition of amyloid fibrils, or both.

To examine this activity of IDX, we first investigated the ability of the compound to bind to PrP amyloid. Serial sections of the cerebral cortex and cerebellum from scrapie-infected hamsters and patients with Creutzfeldt-Jakob disease were incubated with 10^{-7} M aqueous solution of IDX or with the amyloid-binding fluorochrome thioflavine S and were analyzed by fluorescence microscopy (*9*). The comparison of adjacent sections showed that all amyloid deposits revealed by thioflavine S exhibited the characteristic fluorescence of IDX (Fig. 1, B and C).

We then investigated the effects of IDX on experimental scrapie, which is regarded as a model for prion diseases (*1*). Three groups of female Syrian hamsters (10 animals per group) were used for the study. The infected controls were injected intracerebrally with 30 μl of 1% (w/v) brain homogenate obtained from hamsters infected with the 263K strain of scrapie that were in the terminal stage of the disease. The IDX-treated hamsters were injected with the same inoculum, coincubated for 1 hour at room temperature with 2.9 mM IDX before intracerebral inoculation. The uninfected controls were injected with 30 μl of 1% suspension of normal hamster brain. Hamsters infected with scrapie agent coincubated with IDX lived significantly longer than those infected with scrapie alone (Fig. 2A). Thus, although all scrapie-infected hamsters had died by 94 days after infection (mean ± SEM = 88.5 ± 1.9 days), IDX-treated hamsters lived up to 128 days [mean ± SEM = 116 ± 5.6 days; $P < 0.01$, one-way analysis of variance (ANOVA)].

Next, separate groups of hamsters (12

F. Tagliavini, B. Canciani, G. Giaccone, M. Porro, M. Bugiani, P. M.-J. Lievens, O. Bugiani, Istituto Nazionale Neurologico Carlo Besta, via Celoria 11, 20133 Milano, Italy.
R. A. McArthur, T. Bandiera, M. Varasi, P. Cassutti, M. A. Cervini, J. Lansen, C. Post, CNS Research, Pharmacia & Upjohn SpA, viale Pasteur 10, 20014 Nerviano (MI), Italy.
E. Peri, P. Dall'Ara, M. Rocchi, G. Poli, Istituto di Microbiologia e Immunologia Veterinaria, Università degli Studi, via Celoria 10, 20133 Milano, Italy.
G. Forloni and M. Salmona, Istituto di Ricerche Farmacologiche Mario Negri, via Eritrea, 62, 20157 Milano, Italy.
A. Suarato, Oncology Research, Pharmacia & Upjohn SpA, viale Pasteur 10, 20014 Nerviano (MI), Italy.
*To whom correspondence should be addressed.

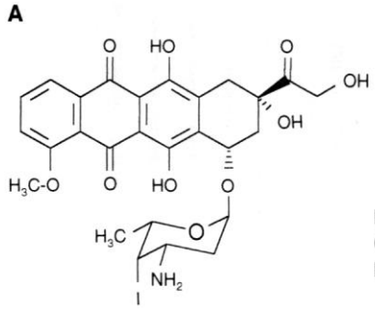

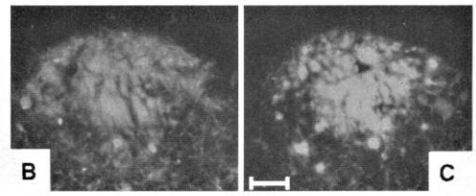

Fig. 1. (**A**) Chemical structure of IDX. (**B**) Binding of IDX and (**C**) thioflavine S to PrP amyloid in brain sections from a patient with Creutzfeldt-Jakob disease. Scale bar, 50 μm.

animals per group) were treated as in the first experiment and were examined at least twice a week to detect the onset and progression of clinical signs of disease (*10*). The key features of scrapie infection were altered reactivity to external stimuli and postural abnormalities with an unsteady gait. The mean time (±SEM) before the appearance of these symptoms was 81.9 ± 2.2 days in infected controls and 102.8 ± 3.8 days in IDX-treated hamsters ($P < 0.01$, one-way ANOVA). The initial phase of the disease was characterized by hyperreactivity to tactile and acoustic stimulation. Subsequently, hamsters began to lose balance and coordination and grew gradually less reactive. The infected controls spent a mean of 85.6 ± 2.5 and 70.0 ± 3.1 days in a "normal" state of posture and balance, respectively, and 94.3 ± 4.9 days without tremors. IDX significantly increased the time spent without postural abnormalities and tremors (Fig. 2C). These changes affected a characteristic escape response when the hamsters were placed in an enclosed area. Before infection, the animals were able to leave a rectangular box within 50 s of a 180-s observation time by climbing over one of the walls. Progressive deterioration of posture and balance in infected hamsters made it more difficult, indeed impossible, for them to climb out of the cage. IDX significantly retarded this deterioration in cage-leaving. The overall average cage-leaving latencies of uninfected controls, infected controls, and IDX-treated hamsters after inoculation were 75 ± 10.3, 163 ± 12.9, and 80.2 ± 16.5 s, respectively (Fig. 2D). Infected control hamsters began to die at a mean of 108.5 ± 2.4 days after infection (Fig. 2B). Those treated with IDX, however, showed significantly longer survival times (125.5 ± 3.1 days; $P < 0.01$, one-way ANOVA), confirming the mortality results seen in the first experiment.

Histological and immunohistochemical analyses (*11*) of brains from four animals of each group culled when behavioral changes were first apparent in the infected controls (days 68 and 80 of the first and second experiments, respectively) showed differences in PrP accumulation, spongiform changes, and astrogliosis. Although the infected controls displayed distinct PrP and glial fibrillary acidic protein (GFAP) immunoreactivity in the cerebral cortex, thalamus, hippocampus, cerebellum, and brain stem, PrP accumulation and astrogliosis were barely detected in the IDX-treated hamsters (Fig. 3). Furthermore, the infected controls showed spongiform changes in the brain stem and, less consistently, in the thalamus, the archicortex, and neocortex, whereas the IDX-treated hamsters did not.

Protein immunoblot analysis (*12*) of brain homogenates with antibodies to PrP confirmed the immunocytochemical observation. The accumulation of proteinase K–resistant PrP-immunoreactive peptides was decreased in IDX-treated hamsters as compared with infected controls (Fig. 4, A and B, upper panels). In contrast, comparable levels of α- and β-tubulin subunits were detected in each group after immunoblot analysis of brain homogenates (Fig. 4, A and B, lower panels). Quantitative evaluation of PrPres, normalized for levels of tubulin, indicated that this decrease was approximately 80% in both experiments. The PrPres-tubulin optical-density ratio between scrapie-infected and IDX-treated hamsters was 4.13 ± 0.22 versus 0.81 ± 0.76 in the first experiment and 3.08 ± 0.36 versus 0.63 ± 0.29 in the second experiment, respectively ($P < 0.01$, paired *t* test). Northern (RNA) blot analysis (*13*) showed similar concentrations of PrP transcript in the brains of uninfected controls, infected controls, and IDX-treated hamsters, which suggests that the decrease in

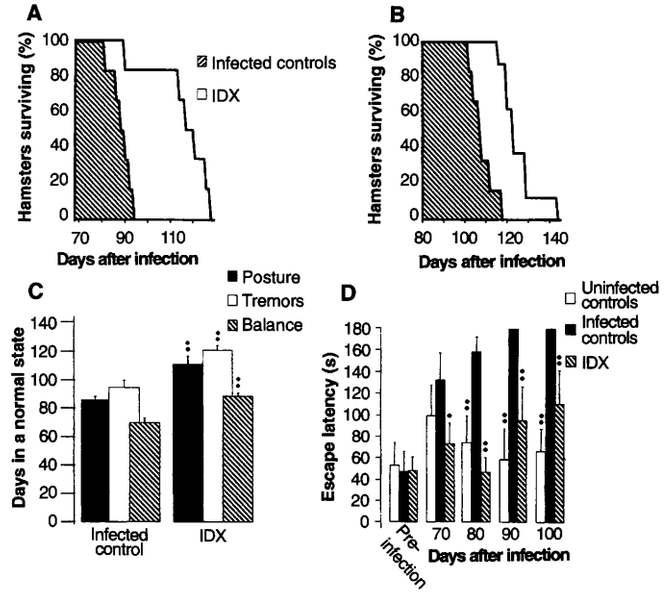

Fig. 2. Effects of IDX on the survival and behavior of Syrian hamsters infected with scrapie (*10*). (**A** and **B**) Survival time of infected controls (shaded area) and of IDX-treated hamsters (white area) in the first (A) and second (B) experiments. Longevity was analyzed by Kaplan-Meier survival analysis. (**C**) Mean number of days (±SEM) the infected controls and IDX-treated hamsters of the second study remained in a state of normal posture and balance and had no tremors (** = $P < 0.01$ versus infected controls, Tukey's *q* method for multiple comparison). (**D**) Mean latency (±SEM) with which uninfected controls, infected controls, and IDX-treated hamsters escaped from an enclosed area (* = $P < 0.05$ and ** = $P < 0.01$ versus infected controls, Tukey's *q* method for multiple comparison).

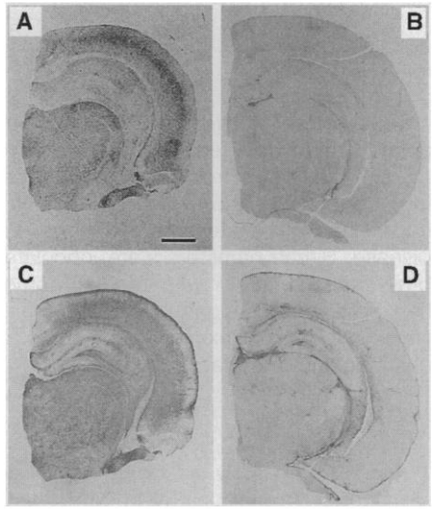

Fig. 3. Effects of IDX on PrP accumulation and astrogliosis in the brain of scrapie-infected hamsters, as revealed by immunohistochemical staining (*11*). Coronal sections of the right cerebral hemisphere of an infected control (**A** and **C**) and an IDX-treated hamster (**B** and **D**) killed at day 80 of the second experiment. The sections are immunostained with antibodies to PrP (A and B) or to GFAP (C and D). Scale bar, 1 mm.

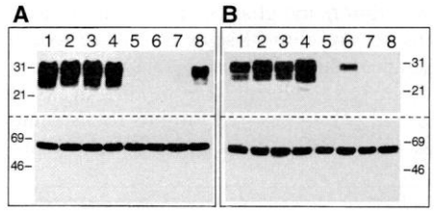

Fig. 4. Effects of IDX on PrPres accumulation in the brain of scrapie-infected hamsters, as revealed by protein immunoblot analysis (*12*). (**A** and **B**) Immunoblots of brain homogenates from hamsters killed at day 68 of the first experiment (A) or day 80 of the second experiment (B). The blots were probed with antibodies to PrP (upper panels) or to tubulin (lower panels). Lanes 1 through 4 correspond to infected controls, and lanes 5 through 8 correspond to IDX-treated hamsters. Numbers at left and right are molecular mass markers, in kilodaltons.

PrPres levels observed in the latter was not due to a decrease in PrP mRNA. Once the disease progressed and hamsters began to die of the infection, the differences between groups in PrP accumulation, spongiform changes, and astrogliosis were no longer apparent.

A wide variety of compounds has been tested in the treatment of prion diseases (*14*). A few of these compounds, particularly amphotericin B and sulfated polyanions, were effective in retarding the appearance of clinical symptoms and prolonging the survival of animals experimentally infected with scrapie (*15*). These compounds are structurally dissimilar and have diverse activity. Amphotericin B, for example, is an antifungal agent, whereas heteropolyanions such as HPA-23 are antivirals. Although these molecules are known to be active at the cell membrane, their mechanism of action in experimental scrapie is still unknown. Other antiviral compounds such as amantadine, vidarabine, and acyclovir have been used in patients with Creutzfeldt-Jakob disease with inconclusive results (*14*).

According to the prion hypothesis, the major component of the agent responsible for transmission of prion disease is PrPres, and prion propagation results from the conformational conversion of normal PrP into an altered form, catalyzed by PrPres (*1*). IDX was administered intracerebrally at the same time as the scrapie agent. This experimental design was dictated by IDX's intrinsic cytotoxicity and pharmacokinetic properties, as well as by its limited ability to pass the blood-brain barrier (*16*). It is conceivable that the delay in PrPres accumulation and the neuropathological and behavioral changes seen may have been a consequence of IDX's binding to abnormal PrP, inhibiting the availability of this protein to act as a template for the conversion of the normal protein. It is unlikely that the anti-scrapie effects of IDX could be due to its cytotoxic properties, because PrP mRNA levels and tubulin concentrations remained unchanged by the treatment. Nevertheless, the possibility that changes in PrP expression could have occurred in IDX-treated animals during the early phase of infection cannot be ruled out.

The results of this study indicate that IDX, although inappropriate for actual treatment of prion diseases because of its cytotoxicity and pharmacokinetic properties, is a prototype of a class of compounds having anti-prion effects. Furthermore, the ability of IDX to bind to different types of amyloid protein (*8*) suggests the possibility that these compounds could also be active in other amyloid-related neurodegenerative diseases.

REFERENCES AND NOTES

1. S. B. Prusiner, *Science* **252**, 1515 (1991); *Annu. Rev. Microbiol.* **48**, 655 (1994).
2. B.W. Caughey *et al.*, *Biochemistry* **30**, 7672 (1991); K.-M. Pan *et al.*, *Proc. Natl. Acad. Sci. U.S.A.* **90**, 10962 (1993); J. Safar, P. P. Roller, D. C. Gajdusek, C. J. Gibbs, *J. Biol. Chem.* **268**, 20276 (1993); S. B. Prusiner *et al.*, *Cell* **35**, 349 (1983); S. J. DeArmond *et al.*, *Ibid.* **41**, 221 (1985).
3. M. E. Bruce, P. A. McBride, C. F. Farquhar, *Neurosci. Lett.* **102**, 1 (1989); S. J. DeArmond *et al.*, in *Prion Diseases of Humans and Animals*, S. B. Prusiner, J. Collinge, J. Powell, B. Anderton, Eds. (Horwood, London, 1992), pp. 483–496; S. J. DeArmond *et al.*, *Proc. Natl. Acad. Sci. U.S.A.* **90**, 6449 (1993); G. Forloni *et al.*, *Nature* **362**, 543 (1993); G. Forloni *et al.*, *Eur. J. Neurosci.* **6**, 1415 (1994); D. R. Brown, B. Schmidt, H. A. Kretzschmar, *Nature* **380**, 345 (1996).
4. L. Ingrosso, A. Ladogana, M. Pocchiari, *J. Virol.* **69**, 506 (1995).
5. B. Caughey and R. E. Race, *J. Neurochem.* **59**, 768 (1992).
6. B. Barbieri *et al.*, *Cancer Res.* **47**, 4001 (1987).
7. L. Gianni, V. Bellotti, A. M. Gianni, G. Merlini, *Blood* **86**, 855 (1995).
8. G. Merlini *et al.*, *Proc. Natl. Acad. Sci. U.S.A.* **92**, 2959 (1995).
9. Samples of the cerebrum and cerebellum from Syrian hamsters infected with the 263K strain of scrapie and from patients with sporadic Creutzfeldt-Jakob disease and amyloid deposits were fixed in 10% formaldehyde and embedded in paraplast. Adjacent sections (8 μm thick) were stained with 1% thioflavine S for amyloid or were incubated with 10^{-7} M aqueous solution of IDX for 1 hour at 37°C, washed for 30 min with 150 mM phosphate-buffer (pH 7.2), and counterstained with Meyer's hematoxylin. The sections were analyzed by fluorescence microscopy (excitation and barrier filters: 436 and 520 nm for thioflavine S; 546 and 580 nm for IDX).
10. The hamsters were housed in groups of four to six animals in a temperature-controlled (20° ± 2°C) quarantined room maintained on a 12-hour light-dark cycle (the light was on from 0600 to 1800). They were allowed free access to food and water, and their body weight was recorded once a week. The animals were observed by research staff who were unaware of the individual treatment conditions, according to a block design in which each block of observations included each treatment condition. The scoring of observational data was carried out as follows. Balance and coordination were evaluated by (i) the ability of the hamster to remain on a narrow plank (a ruler) and (ii) the ability to land on four paws after falling from a thin wire. Posture and tremors were evaluated by observation. The behaviors were scored according to discrete item-ordinate scales as follows. Balance: 0, normal; 1, impaired; 2, unstable; and 3, loss. Posture: 0, normal; 1, abnormal; 2, limbs abducted; and 3, hunchback. Tremors: 0, absent; 1, mild; 2, present; and 3, increased. In order to quantify and analyze these behaviors, the following convention was adopted: The experiment was operationally defined as the period from the day of infection to the day of death of the last scrapie-infected hamster (day 144 after infection). The data from hamsters killed for neuropathological and biochemical examination were excluded from the analysis, and death was considered a behavioral state within the definition of the experiment. The number of days in which each hamster was in a particular state of behavior (normal, increased, reduced, absent, or dead) was counted. As behavioral observations took place at intervals rather than daily, an estimate of the behavioral stage between observations was made by assigning the same score within each day if the score at each limiting observational day was the same. Otherwise, if the behavioral score between one observational day and another changed, then half of the intervening days were assigned the lower score and half of the intervening days were assigned the higher score. These data were then analyzed according to a split-plot factorial design, with the treatment group being the independent factor and the state of behavior factor being repeated. The cage leaving behavior of the hamsters was observed and recorded by video in a rectangular cage (22 by 36 by 12 cm). Recording sessions were carried out before infection and at various days after infection. The observation period lasted a maximum of 180 s. Post-hoc paired comparisons between means were evaluated by Tukey's q method for multiple comparisons, where * = $P < 0.05$ and ** = $P < 0.01$ from infected controls.
11. For neuropathological and biochemical examination, four hamsters from each group were killed (according to the Policy on the Use of Animals in Neuroscience Research of the Society for Neuroscience) when behavioral changes were first apparent in the infected controls. The remaining hamsters were analyzed after dying at the terminal stage of the disease. The left cerebral hemisphere was frozen and stored at −80°C; the right hemisphere was fixed in Carnoy solution, cut coronally at four standard levels, and embedded in paraplast. Serial sections (8 μm thick) from each block were stained with hematoxylin-eosin and thioflavine S or incubated with a monoclonal antibody (mAb) to GFAP (Boehringer-Mannheim, Germany) (ratio, 1:100) or the mAb 3F4 (ratio, 1:200), which recognizes an epitope including residues 108 to 111 of hamster PrP. Immunoreactions were revealed by the peroxidase-antiperoxidase method with the use of goat anti-mouse immunoglobulins, PAP complex (DAKO, Denmark), and 3-3′-diaminobenzidine. Negative control sections were incubated with normal mouse serum as primary antibody. The specificity of PrP immunoreactivity was verified by absorption. The antibody 3F4 was incubated with a synthetic peptide homologous to residues 101 to 119 of human PrP (10 mM) for 1 hour at 37°C and then overnight at 4°C. After centrifugation at 15,000*g* for 15 min, the supernatant was used as primary antibody.
12. A 10% (w/v) homogenate of the left cerebral hemisphere from each hamster was prepared in 100 mM NaCl, 10 mM EDTA, 0.5% NP-40, 0.5% sodium deoxycholate, and 10 mM tris (pH 7.4). After centrifugation at 1000*g* for 10 min, the protein concentration in the supernatant was determined by the bicinchoninic acid assay (Pierce, USA). Samples equivalent to 100 μg of protein were mixed with equal volumes of twice the concentration of Laemmli sample buffer and incubated with proteinase K (20 μg/ml) for 1 hour at 37°C. Proteolysis was terminated by the addition of phenylmethylsulfonyl fluoride (1 mM final concentration). The samples were fractionated on 12.5% SDS-polyacrylamide minigels under reducing conditions, electrophoretically transferred to polyvinylidene difluoride membranes (Immobilon, Millipore, USA), and probed with the antibody 3F4 (ratio, 1:50,000) as described previously (*17*). Further aliquots of the original samples were probed with mAbs to α- and β-tubulin subunits (Amersham, UK) (ratio, 1:5000). Immunoreactive bands were visualized with enhanced chemoluminescence (Amersham), and quantified by densitometry with a Mitsubishi Video Copy Processor (Model P68E), a IV-530 Contour Synthesizer (FOR-A Co. Limited, France), and the Bio-Profil package of softwares (Vilber-Lourmat, France). The specificity of the reactions was checked with the use of normal mouse serum and absorbed 3F4 as primary antibodies. Densitometric data were analyzed according to ANOVA, examining the effects of IDX across the two experiments on the resolved optical density of PrP-immunoreactive bands normalized for tubulin. The significance of difference from respective controls was assessed by paired t test.
13. Total RNA was isolated from brain homogenates of uninfected controls, infected controls, and IDX-treated hamsters by a single-step method, with the use of the ultraspec RNA isolation system (Biotecx). Fifteen μg of RNA from each sample was fractionated by MOPS-EDTA agarose gel electrophoresis and transferred to Hybond-N+ membranes (Amersham). The filters were hybridized with human PrP cDNA that was labeled to a specific activity >1 × 10^8 cpm/μg, using [^{32}P]deoxycytidine triphosphate by the random primer labeling procedure (*18*). The membranes were washed

and exposed to film at −70°C. β-actin mRNA was used as an internal standard.
14. P. Brown, *Antiviral Chem. Chemother.* **1**, 75 (1990); ——— in *Antiviral Agents: The Development and Assessment of Antiviral Chemotherapy*, H. J. Field, Ed. (CRC Press, Boca Raton, FL, 1988), vol. 2, pp. 13–28.
15. B. Ehlers and H. Diringer, *J. Gen. Virol.* **65**, 1325 (1984); C. F. Farquhar and A. G. Dickinson, *ibid.* **67**, 463 (1986); R. H. Kimberlin and C. A. Walker, *Antimicrob. Agents Chemother.* **30**, 409 (1986); M. Pocchiari, S. Schmittinger, C. Masullo, *J. Gen. Virol.* **68**, 219 (1987); Y. G. Xi, L. Ingrosso, A. Ladogana, C. Masullo, M. Pocchiari, *Nature* **356**, 598 (1992); R. H. Kimberlin and C. A. Walker, *Arch. Virol.* **78**, 9 (1993); K. T. Adjou *et al.*, *Antimicrob. Agents Chemother.* **39**, 2810 (1995).
16. F. Fomelli, R. Carsana, C. Pollini, *Cancer Res.* **47**, 5401 (1987).
17. F. Tagliavini *et al.*, *Cell* **79**, 695 (1994).
18. J. Sambrook, E. F. Fritsch, T. Maniatis, in *Molecular Cloning: A Laboratory Manual* (Cold Spring Harbor Laboratory Press, Cold Spring Harbor, NY, 1989).
19. We thank R. J. Kascsak for providing the antibody 3F4, L. Frigerio for preparation of histological sections, and M. Rochetti for statistical advice. Partially supported by the Italian Ministry of Health, Department of Social Services, Telethon-Italy (grant E.250) and the Consiglio Nazionale delle Ricerche (grant ST/74).

9 January 1997; accepted 25 March 1997

A Membrane Network for Nutrient Import in Red Cells Infected with the Malaria Parasite

Sabine A. Lauer, Pradipsinh K. Rathod, Nafisa Ghori, Kasturi Haldar*

The human malaria parasite *Plasmodium falciparum* exports an interconnected network of tubovesicular membranes (the TVM) that extends from the parasite's vacuolar membrane to the periphery of the red cell. Here it is shown that extracellular solutes such as Lucifer yellow enter the TVM and are delivered to the parasite. Blocking the assembly of the network blocked the delivery of exogenous Lucifer yellow, nucleosides, and amino acids to the parasite without inhibiting secretion of plasmodial proteins. These data suggest that the TVM is a transport network that allows nutrients efficient access to the parasite and could be used to deliver antimalarial drugs directly into the parasite.

Malaria afflicts 200 million to 300 million people and kills over 1 million children each year. The most fatal form of the disease is caused by the protozoan parasite *Plasmodium falciparum*. During its asexual cycle the parasite invades and develops in a vacuole in the mature erythrocyte, a cell devoid of all intracellular organelles and incapable of de novo protein synthesis and membrane turnover (*1*, *2*). In order to survive, the parasite exports antigens and imports extracellular nutrients (*3*–*5*) across the intraerythrocytic space by mechanisms that are largely unknown. Within 33 hours of infection the parasite induces the formation of the TVM that emerges from the parasitophorous vacuolar membrane and extends out to the erythrocyte membrane (*6*, *7*), suggesting that it may be a transport organelle.

TVM assembly can be blocked by inhibition of a resident parasite sphingomyelin synthase (called the sensitive sphingomyelin synthase or SSS) by *dl*-threo-1-phenyl-2-palmitoylamino-3-morpholino-1-propanol (PPMP; Fig. 1) (*8*). Normal cells have shown a highly tubular network with a few large loops (Fig. 1A). PPMP-treated cells (Fig. 1B) were found to contain vesicles or rodlike elements, associated with the red cell membrane, free in the cytoplasm or in close association with the parasite. Few of the intraerythrocytic structures appeared to be interconnected, suggesting that the network is either highly constricted in regions that do not stain with Bodipy-ceramide, or it is fragmented.

To determine whether the state of TVM organization influences the transport properties of infected red cells, we incubated control (untreated) and PPMP-treated cells with the fluorescent solute Lucifer yellow (LY), which enters infected (but not uninfected) red cells by a parasite-induced, energy-dependent process (*9*). In mammalian cells LY is a marker for fluid phase pinocytosis; however, there is no endocytic activity at the infected red cell membrane (*10*, *11*). In a normal infected red cell, LY was detected in interconnected tubules and vesicles of the TVM and within the parasite (Fig. 1C). Labeled network structures extended along the periphery of the red cell across the intraerythrocytic space and back to the parasite. PPMP-treated cells appeared to be blocked in the intraerythrocytic delivery and accumulation of LY (Fig. 1D). Removal of PPMP restored TVM development (*8*) and the levels of LY transport and accumulation seen in untreated cells (*12*). PPMP does not block the channel or transporter for LY at the infected red cell membrane (*12*). Together, these data suggest that LY is delivered by the TVM to the parasite.

We next investigated whether other charged, low molecular mass solutes such as nucleosides, amino acids, and their toxic derivatives are also transported by the TVM by comparing parasite-induced accumulation of radiolabeled analogs in PPMP-treated and untreated cells. An important extracellular solute for parasite growth is the purine nucleoside adenosine. The parasite needs purines for growth but cannot synthesize them de novo. The uninfected erythrocyte has an endogenous nucleoside transporter that can be blocked by derivatives of 6-thiopurine nucleosides such as nitrobenzyl thioinosine (NBMPR); however, these compounds do not block parasite-induced nucleoside accumula-

Table 1. Inhibition of parasite-induced solute accumulation and use in infected red cells. Infected erythrocytes (at 10 to 20% parasitemia) treated with 5 μM PPMP for 36 hours were washed free of serum and incubated with the indicated radiolabeled substrates (*14*). The accumulation of [^{3}H]adenosine or [^{3}H]thymidine was measured over 30 s at room temperature. NBMPR (20 μM) was used to inhibit the endogenous red cell nucleoside transporter. Control cells were not treated with PPMP. Where indicated, 0.01% saponin was added. The accumulation of [^{3}H]orotic acid and [^{3}H]glutamate was measured over 30 min at 37°C. PPMP treatment had no effect on the uptake of any radiolabeled compound into uninfected red cells. The incorporation of [^{3}H]adenosine and [^{3}H]orotic acid was measured over 24 hours, after which the cells were harvested on glass fiber filters and the counts determined (*8*, *14*). These incorporation assays were carried out in the absence of NBMPR. The incorporation of [^{3}H]glutamate over 24 hours at 37°C was determined by measuring the acid-insoluble radioactivity precipitated on 3 MM Whatman filters (*17*, *14*). n.a., not applicable.

Substrate	Solute accumulation (10^{-5} nmol per 5×10^7 parasites)		Inhibition of accumulation (%)	Inhibition of incorporation (%)
	−PPMP	+PPMP		
[^{3}H]Adenosine	7.8	3.1	60 ± 20	97 ± 2
[^{3}H]Adenosine + saponin	6.2	5.6	9 ± 4	3 ± 2
[^{3}H]Orotic acid	17	1.5	91 ± 13	98 ± 1
[^{3}H]Thymidine	46	10	78 ± 6	n.a.
[^{3}H]Glutamate	14	3.6	74 ± 20	91 ± 5

S. A. Lauer, N. Ghori, K. Haldar, Department of Microbiology and Immunology, Stanford University School of Medicine, Stanford, CA 94305–5402, USA.
P. K. Rathod, Department of Biology, Institute for Biomolecular Studies, The Catholic University of America, Washington, DC 20064, USA.
*To whom correspondence should be addressed.